The EUMETSAT Network of Satellite Application Facilities

H SAF

Support to Operational Hydrology and Water Management

Italian Meteorological Service

Italian Department of Civil Defence

Algorithm Theoretical Definition Document (ATDD) for product

SN-OBS-2 - Snow status (dry/wet) by MW radiometry

Zentralanstalt für Meteorologie und Geodynamik

Vienna University of Technology Institut für Photogrammetrie und Fernerkundung

Royal Meteorological Institute of Belgium

European Centre for Medium-Range Weather Forecasts

Finnish Meteorological Institute

Finnish Environment Institute

Helsinki University of Technology

Météo-France

CNRS Laboratoire Atmosphères, Milieux, Observations Spatiales

CNRS Centre d'Etudes Spatiales de la BIOsphere

Bundesanstalt für Gewässerkunde

Hungarian Meteorological Service

CNR - Istituto Scienze dell'Atmosfera e del Clima

Università di Ferrara

Institute of Meteorology and Water Management

Romania National Meteorological Administration

Slovak Hydro-Meteorological Institute

Turkish State Meteorological Service

Middle East Technical University

Istanbul Technical University

Anadolu University

31 August 2010

Algorithm Theoretical Definition Document ATDD-11
Product SN-OBS-2
Snow status (dry/wet) by MW radiometry

INDEX

List of Tables

List of Figures

Acronyms

AMSR-E	Advanced Microwave Scanning Radiometer for EOS (on EOS-Aqua)
ATDD	Algorithms Theoretical Definition Document
AU	Anadolu University (in Turkey)
AVHRR	Advanced Very High Resolution Radiometer (on NOAA and MetOp)
BfG	Bundesanstalt für Gewässerkunde (in Germany)
CAF	Central Application Facility (of EUMETSAT)
CESBIO	Centre d'Etudes Spatiales de la BIOsphere (of CNRS, in France)
CM-SAF	SAF on Climate Monitoring
CNMCA	Centro Nazionale di Meteorologia e Climatologia Aeronautica (in Italy)
CNR	Consiglio Nazionale delle Ricerche (of Italy)
CNRS	Centre Nationale de la Recherche Scientifique (of France)
DMSP	Defence Meteorological Satellite Program
DPC	Dipartimento Protezione Civile (of Italy)
DWD	Deutscher Wetterdienst
ECMWF	European Centre for Medium-range Weather Forecasts
EOS	Earth Observing System (*Terra*, *Aqua*, *Aura*)
EUM	Short for EUMETSAT
EUMETCast	EUMETSAT's Broadcast System for Environmental Data
EUMETSAT	European Organisation for the Exploitation of Meteorological Satellites
FAR	False Alarm Rate
FMI	Finnish Meteorological Institute
FTP	File Transfer Protocol
GEO	Geostationary Earth Orbit
GOES	Geostationary Operational Environmental Satellite
GRAS-SAF	SAF on GRAS Meteorology
H-SAF	SAF on Support to Operational Hydrology and Water Management
IFOV	Instantaneous Field Of View
IMWM	Institute of Meteorology and Water Management (in Poland)
IPF	Institut für Photogrammetrie und Fernerkundung (of TU-Wien, in Austria)
IR	Infra Red
IRM	Institut Royal Météorologique (of Belgium) (alternative of RMI)
ISAC	Istituto di Scienze dell'Atmosfera e del Clima (of CNR, Italy)
ITU	İstanbul Technical University (in Turkey)
LATMOS	Laboratoire Atmosphères, Milieux, Observations Spatiales (of CNRS, in France)
LEO	Low Earth Orbit
LSA-SAF	SAF on Land Surface Analysis
Météo France	National Meteorological Service of France
METU	Middle East Technical University (in Turkey)
MODIS	Moderate-resolution Imaging Spectro-radiometer (on EOS Terra and Aqua)
MW	Micro Wave
NASA	National Aeronautical and Space Administration (in USA)
NMA	National Meteorological Administration (of Romania)
NOAA	National Oceanic and Atmospheric Administration (Agency and satellite)
NWC	Nowcasting
NWC-SAF	SAF in support to Nowcasting & Very Short Range Forecasting
NWP	Numerical Weather Prediction
NWP-SAF	SAF on Numerical Weather Prediction
O3M-SAF	SAF on Ozone and Atmospheric Chemistry Monitoring
OMSZ	Hungarian Meteorological Service
OSI-SAF	SAF on Ocean and Sea Ice
Pixel	Picture element

POD	Probability of Detection
PUM	Product User Manual
PVR	Product Validation Report
REP-3	H-SAF Products Validation Report
RMI	Royal Meteorological Institute (of Belgium) (alternative of IRM)
SAF	Satellite Application Facility
SD	Snow Depth
SEVIRI	Spinning Enhanced Visible and Infra-Red Imager (on Meteosat from 8 onwards)
SHMÚ	Slovak Hydro-Meteorological Institute
SMMR	Scanning Multichannel Microwave Radiometer (on Nimbus 7 and SeaSat)
SSM/I	Special Sensor Microwave / Imager (on DMSP up to F-15)
SSMIS	Special Sensor Microwave Imager/Sounder (on DMSP starting with S-16)
SYKE	Suomen ympäristökeskus (Finnish Environment Institute)
TKK	Teknillinen korkeakoulu (Helsinki University of Technology)
TSMS	Turkish State Meteorological Service
TU-Wien	Technische Universität Wien (in Austria)
UniFe	University of Ferrara (in Italy)
VIS	Visible
ZAMG	Zentralanstalt für Meteorologie und Geodynamik (of Austria)

1. The EUMETSAT Satellite Application Facilities and H-SAF

The "*EUMETSAT Satellite Application Facility on Support to Operational Hydrology and Water Management (H-SAF)*" is part of the distributed application ground segment of the "*European Organisation for the Exploitation of Meteorological Satellites (EUMETSAT)*". The application ground segment consists of a "*Central Application Facility (CAF)*" and a network of eight "*Satellite Application Facilities (SAFs)*" dedicated to development and operational activities to provide satellite-derived data to support specific user communities. See ***Fig. 01***.

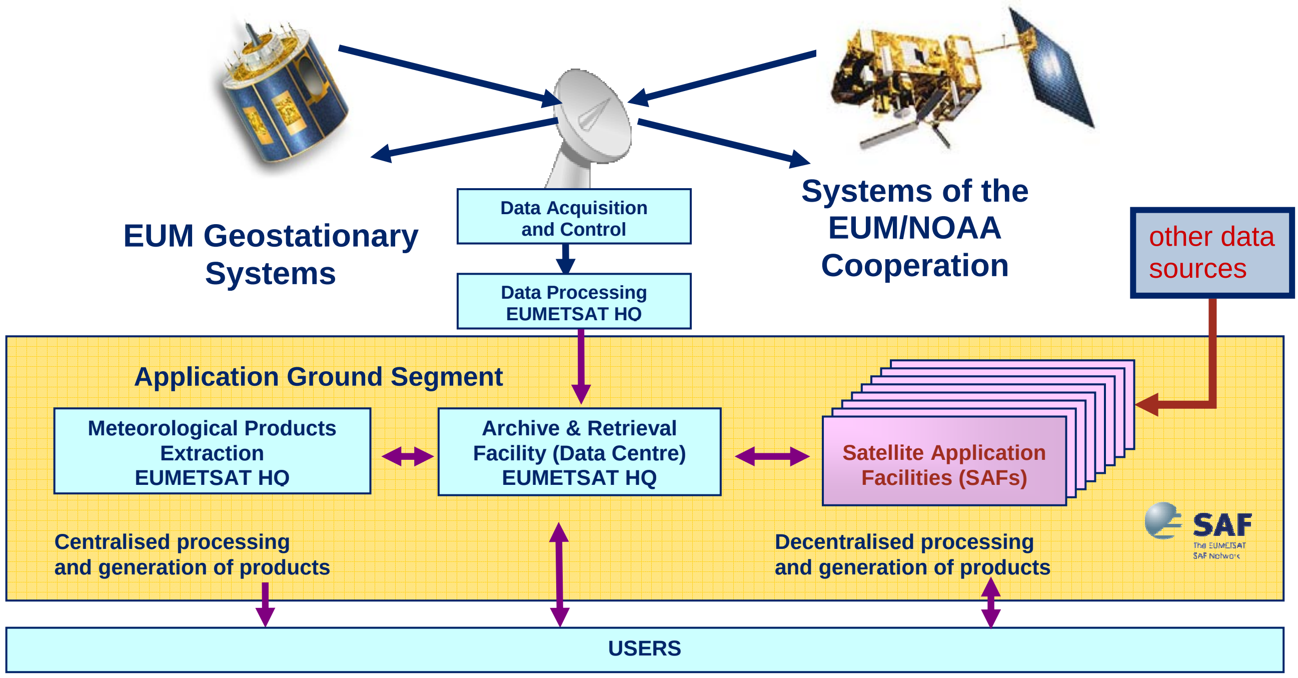

Fig. 01 - Conceptual scheme of the EUMETSAT application ground segment.

Fig. 02 reminds the current composition of the EUMETSAT SAF network (in order of establishment).

NWC SAF	OSI SAF	O3M SAF	CM SAF	NWP SAF	GRAS SAF	LSA SAF	H SAF
Nowcasting & Very Short Range Forecasting	Ocean and Sea Ice	Ozone & Atmospheric Chemistry Monitoring	Climate Monitoring	Numerical Weather Prediction	GRAS Meteorology	Land Surface Analysis	Operational Hydrology & Water Management

Fig. 02 - Current composition of the EUMETSAT SAF network (in order of establishment).

The H-SAF was established by the EUMETSAT Council on 3 July 2005; its Development Phase started on 1st September 2005 and ends on 31 August 2010. The list of H-SAF products is shown in ***Table 01.***

Table 01 - List of H-SAF products

Code	Acronym	Product name
H01	PR-OBS-1	Precipitation rate at ground by MW conical scanners (with indication of phase)
H02	PR-OBS-2	Precipitation rate at ground by MW cross-track scanners (with indication of phase)
H03	PR-OBS-3	Precipitation rate at ground by GEO/IR supported by LEO/MW
H04	PR-OBS-4	Precipitation rate at ground by LEO/MW supported by GEO/IR (with flag for phase)
H05	PR-OBS-5	Accumulated precipitation at ground by blended MW and IR
H06	PR-ASS-1	Instantaneous and accumulated precipitation at ground computed by a NWP model
H07	SM-OBS-1	Large-scale surface soil moisture by radar scatterometer
H08	SM-OBS-2	Small-scale surface soil moisture by radar scatterometer
H09	SM-ASS-1	Volumetric soil moisture (roots region) by scatterometer assimilation in NWP model
H10	SN-OBS-1	Snow detection (snow mask) by VIS/IR radiometry
H11	SN-OBS-2	Snow status (dry/wet) by MW radiometry
H12	SN-OBS-3	Effective snow cover by VIS/IR radiometry
H13	SN-OBS-4	Snow water equivalent by MW radiometry

2. Introduction to product SN-OBS-2

2.1 Sensing principle

Product SN-OBS-2 (*Snow status (dry/wet) by MW radiometry*) is fundamentally based on the AMSR-E microwave radiometer being flown on EOS-Aqua. In case of failure of AMSR-E or of EOS-Aqua, SSM/I and SSMIS flown on the DMSP satellites will be used (with much worse resolution). These conical scanners provide images with constant zenith angle, that implies constant optical path in the atmosphere and homogeneous impact of the polarisation effects (see ***Fig. 03***).

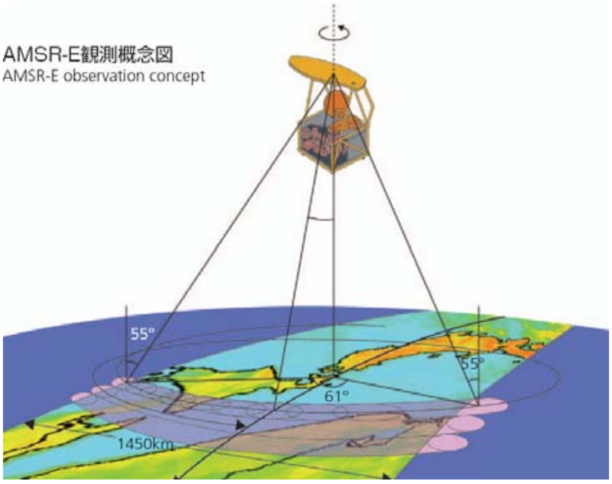

Fig. 03 - Geometry of conical scanning for AMSR-E.

Also, conical scanning provides constant resolution across the image, though changing with frequency. It is noted that the IFOV is elliptical, with major axis elongated along the viewing direction and the minor axis along-scan, approximately 2/3 of the major. As for the 'pixel', i.e. the area subtended as a consequence of the bi-dimensional sampling rate, the sampling distance along the satellite motion, i.e. from scan line to scan line, is invariably 10 km, dictated by the satellite velocity on the ground and the scan rate. Along scan, the sampling rate is 10 km for all channels except 89 GHz where it is 5 km.

The EOS-Aqua satellite is managed by NASA. Direct reception is possible, but AMSR-E data are generally acquired by ftp from NASA archives. The delay from the observation time is around 6 h, with considerable fluctuations due to the availability of the NASA ftp server.

For more information, please refer to the Products User Manual (specifically, volume PUM-11).

2.2 Main operational characteristics

The operational characteristics of SN-OBS-2 are discussed in PUM-11. Here are the main highlights.

The horizontal resolution (Δx) descends from the AMSR-E Instantaneous Field of View (*IFOV*) that, at the frequencies utilised, 18.7 and 36.5 GHz, is ~ 20 km and ~ 11 km respectively. The lower frequency dominates. Sampling is made at 0.25-degree intervals. Thus:

- resolution Δx ~ 20 km - sampling distance: ~ 20 km.

The *observing cycle (Δt)*. The AMSR-E observing cycle is 24 h, and anyway the product is outputted each 24 hours in order to be sure, from SN-OBS-1 (Snow mask), of snow existence. Thus:

- observing cycle: Δt = 24 h.

The *timeliness (δ)*. For a product resulting by assembling data collected until a fixed time of the day, the time of observation may change across the scene (some area may have been observed early in the time window, thus up to 24-h old at the time of dissemination; some very recently, just before product dissemination). The average delay is therefore δ = 12 h. Conclusion:

- timeliness δ ~ 12 h.

The *accuracy*, for a binary product (snow / no-snow), is quoted as Probability Of Detection (POD) and False Alarm Rate (FAR), i.e. the success in distinguish wet snow from dry snow. It is evaluated *a-posteriori* by means of the validation activity. See Product Validation Report PVR-11.

2.3 Architecture of the products generation chain

The architecture of the SN-OBS-2 product generation chain is shown in ***Fig. 04***

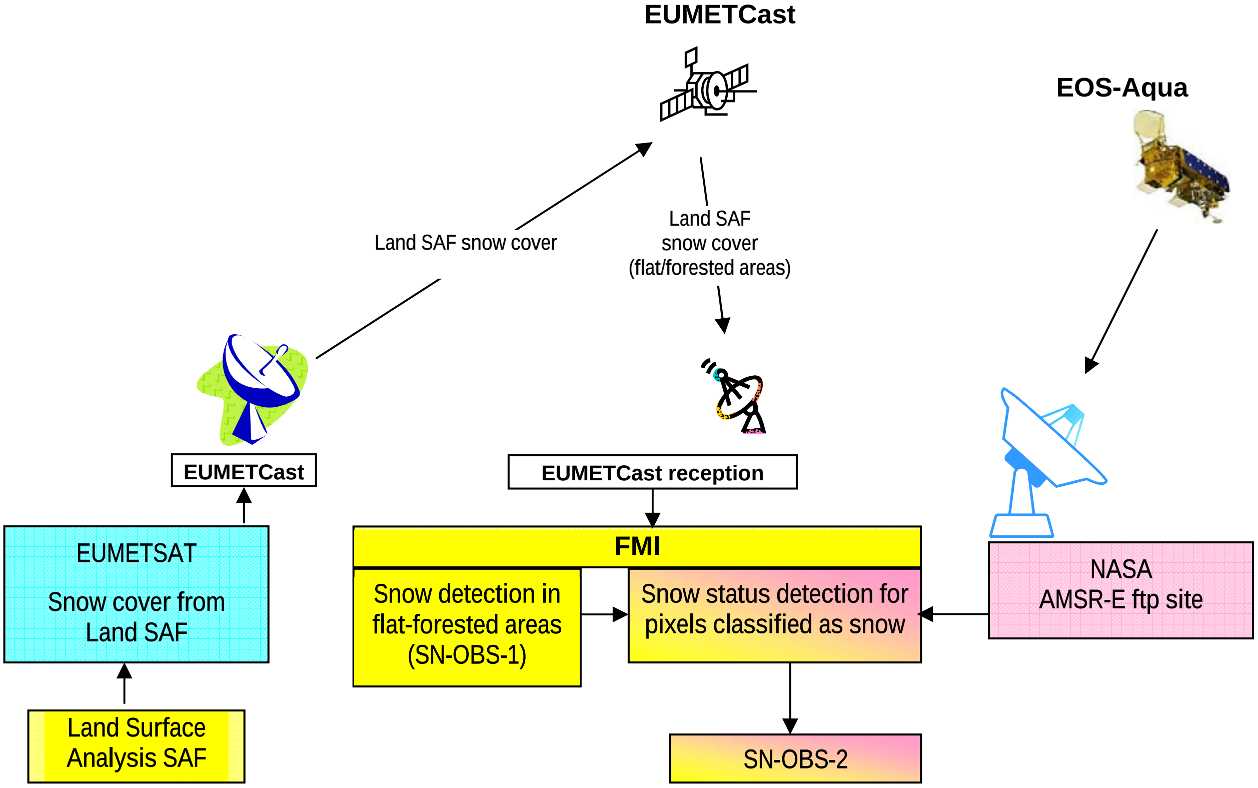

Fig. 04 - Conceptual architecture of the SN-OBS-2 chain.

It is noted that the dependence of product SN-OBS-2 from preventive classification by SN-OBS-1 implies that the product, although in principle possible to be generated after each EOS-Aqua pass (being AMSR-E all-weather and available night and day), in practice has to follow the SN-OBS-1 generation rate, i.e. 24 hours. Anyway, the retrieval of data from the NASA archive introduces delays of several hours.

Unlike the other H-SAF snow products, that are processed at two locations (FMI for flat/forested areas, TSMS for mountainous areas), SN-OBS-2 is produced only at FMI and, although covers the full H-SAF area, only the flat/forested areas are committed for nominal quality. The product is held on the FMI and CNMCA servers.

2.4 Product development team

Names and coordinates of the main actors for SN-OBS-2 algorithm development and integration are listed in ***Table 02***.

Table 02 - Development team for product SN-OBS-2

Jouni Pulliainen (Leader)	Finnish Meteorological Institut (FMI)	Finland	jouni.pulliainen@fmi.fi
Panu Lahtinen			panu.lahtinen@fmi.fi
Juha-Petri Kärnä	Helsinki University of Technology (TKK)		juha-petri.karna@ymparisto.fi
Sampsa Koponen			sampsa.koponen@tkk.fi

3. Processing concept

Fig. 05 illustrates the flowchart of processing chain for snow status retrieval.

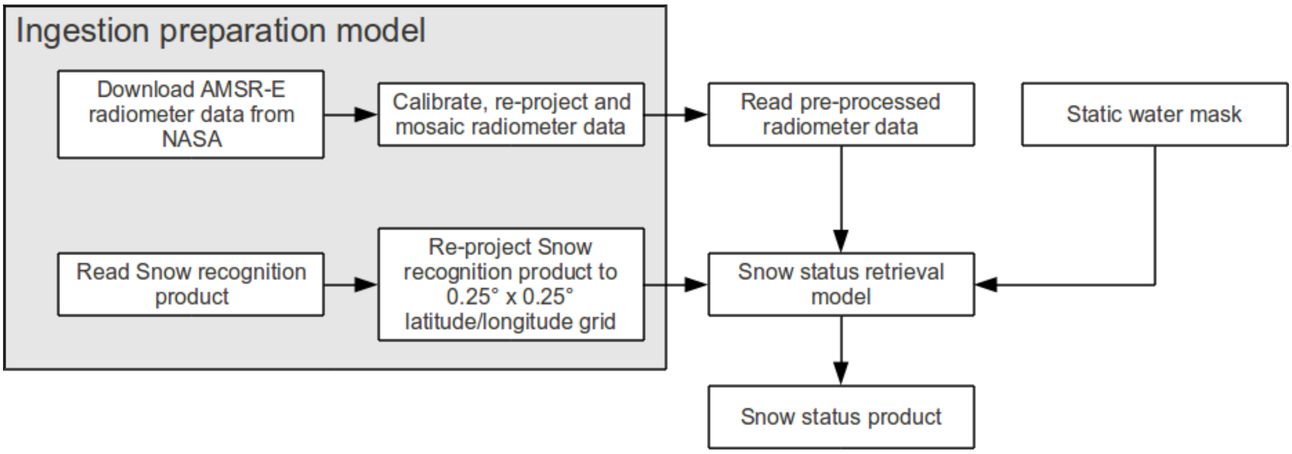

Fig. 05 - Flow chart of the snow status recognition processing chain.

The base for the product is the snow recognition product (see Algorithm Theoretical Definition Document, ATDD-10), which is used as a marker to find snow regardless of the dryness or wetness. As the snow recognition product is in different projection, it is reprojected to the 0.25° x 0.25° equal latitude/longitude grid of the end product. In this stage, the product values "snow" in the snow recognition product is changed to "wet snow".

Parallel to this, AMSR-E radiometer data are processed. After each new radiometer swath that is downloaded from NASA ftp, the data are rectified and mosaicked to cover the H-SAF domain. A watermask is included to the radiometer data, and this is used for the pixels having data. A static watermask is used to fill in the gaps between different satellite overpasses.

These data are fed to the snow status retrieval model, which applies the formulae shown in section 4.2 to retrieve the pixels with dry snow, and corresponding pixels in the output are updated to show this status.

4. Algorithms description

4.1 Ingestion preparation model

Ingestion preparation model, marked in gray in Fig. 05, will prepare the pre-processed data to be used by the snow status retrieval model.

Both, the radiometer data and the snow recognition product (see ATDD-10) are prepared for use. The snow recognition product is re-projected to the correct projection, and the "snow" class is changed to "wet snow".

For radiometer data, the preparation starts with re-projection of the satellite count values and the associated water fraction data. The count values are then calibrated for each used channel (see section 4.2), and saved to the channel specific daily files. As the data are processed in sequential order, the most recent data replaces the data from the previous overpasses, also increasing the spatial coverage obtained.

4.2 Snow status retrieval model

Snow status retrieval is based on snow depth algorithm presented by Rees 2005:

$$SD = 15.9\ (T_{19H} - T_{37H}), \qquad (1)$$

where T_{19H} and T_{37H} are brightness temperatures seen using horizontal polarisation and 19 and 37 GHz channels, respectively. The criteria for dry snow are:

$$SD > 80 \text{ mm and } T_{37H} < 250 \text{ K and } T_{37H} < 240 \text{ K}. \qquad (2)$$

If these criteria are not met, the value present in the snow recognition product based data are used. This is due to that it is not possible to discriminate wet snow from wet ground, as the liquid water dominates the emissivity of the media in both cases.

Since the snow recognition product, used to augment microwave data, is based on optical data, values for wet snow can only be present on clear-sky conditions with sufficient sun elevation. This rules out not only the deepest winter in the north (see section 5 for example), but also a lot of the snow season in the whole H-SAF domain, as the cloudiness is dominant during winter months.

The recognition of dry snow from snow pack shallower than 80 mm gets more and more unreliable due to high penetration depth of microwave frequencies in dry snow, and the emission from the underlying soil starts to affect the observed brightness temperature.

4.3 Algorithms validation/heritage

Remote sensing of snow using microwave radiometers has a long history, since microwave instruments have flown in satellites since 1970s.

Theoretically, the change from dry snow to wet snow should be relatively easy to detect since the microwave emission changes quite much due to the large change in dielectric constant. In practice the change is not so clear due to inhomogenities of the snow cover, varied land cover, vegetation effects etc.. Also the relatively coarse resolution of the AMSR-E product (10 km at 37 GHz, 20 km at 19 GHz) is a little problematic due to mixed-pixel effects.

The aforementioned algorithm is published in 2002 by Hall et al. and referenced in literature, for example in a book of Rees 2005. The algorithm is a modification of the algorithm of Chang et al. 1987.

Although the algorithm is intended for global snow mapping, it requires some modification for use at high altitude. For example in the Himalayas, Saraf et al. 1999 proposed the following algorithm for SMMR data:

$$SD = 20\ (T_{19H} - T_{37H}) - 80.$$

An automated global snow cover mapping based on multi-source data (GOES, AVHRR, SSM/I) is reported to coincide with manual classification of multi-source data within 85 % of time (Rees 2005).

Hall et al. 2007 have studied the relative performance of snow mapping using optical sensors (MODIS) and passive microwave instruments (AMSR-E). One thing they noticed is that the optical sensors work better at the start of the winter while microwave sensors work better from the mid winter onwards. But the overall result was that microwave data give important contribution to the optical data suffering from clouds.

5. Examples of snow status maps

Fig. 06 and ***Fig. 07*** /same as in PUM-11) show examples of SN-OBS-2 products and corresponding SN-OBS-1. Fig. 06 refers to "deep" winter, with mostly dry snow, Fig. 07 showing more melting. Maps are in *equal latitude/longitude grid* with sampling intervals of 0.25 degrees.

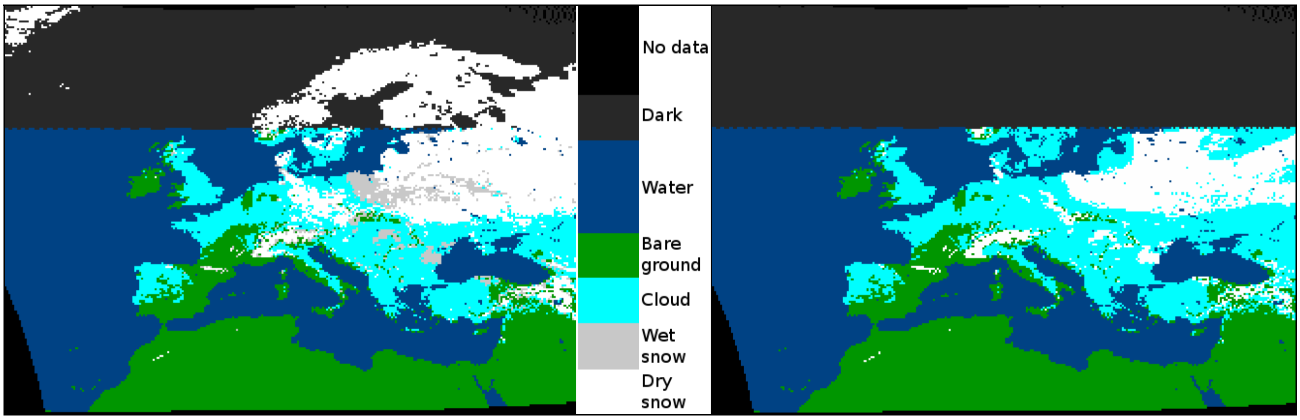

Fig. 06 - Snow map as in SN-OBS-2 (left) from AMSR-E and SN-OBS-1 (right) from SEVIRI. 24-h composite. 22 January 2010.

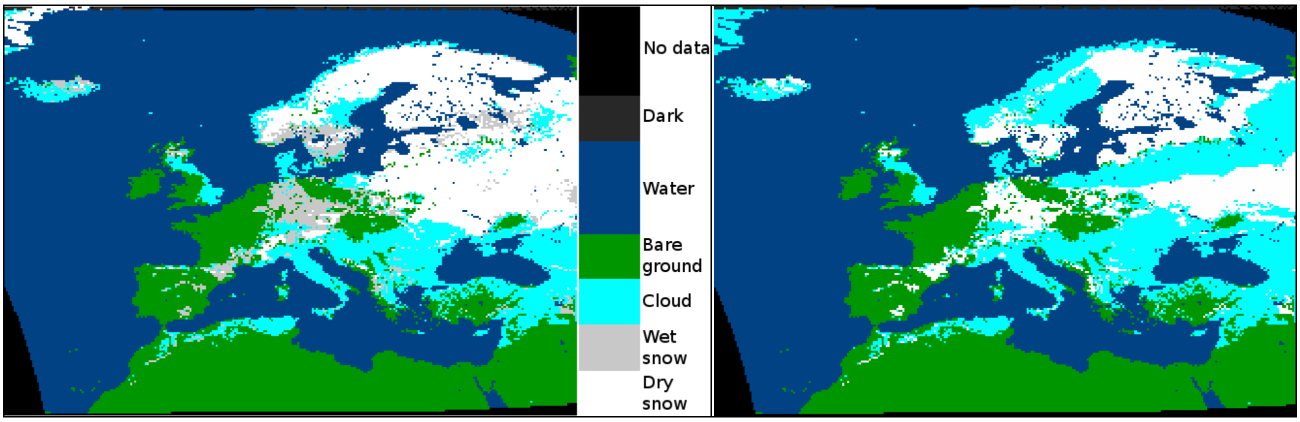

Fig. 07 - Snow map as in SN-OBS-2 (left) from AMSR-E and SN-OBS-1 (right) from SEVIRI. 24-h composite. 09 March 2010.

References

Chang A.T.C., J.L. Foster and D.K. Hall, 1987: "Nimbus-7 SMMR-derived global snow cover parameters". *Ann. Glaciol.*, 9, 39-44.

Hall D.K., P.M. Montesano, J.L. Foster, G.A. Riggs, R.E.J. Kelly and K. Czajkowski, 2007: "Preliminary Evaluation of the AFWA-NASA Blended Snow-Cover Product over the Lower Great Lakes region". *64th Eastern Snow Conference, St. Johns, Newfoundland, Canada, 2007*.

Hall D.K., R.E.J. Kelly, G.A. Riggs, A.T.C. Chang, and J.L. Foster. 2002: "Assessment of the relative accuracy of hemispheric-scale snow-cover maps". *Annals of glaciology* 34:24-30.

Rees W.G, 2005: "*Remote sensing of snow and ice*." CRC Press. 285 pages. ISBN-0415298318.

Saraf A.K., J.L. Foster, P. Singh and S. Tarafdar, 1999: "Passive microwave data for snow-depth and snow-extent estimations in Himalayan mountains". *International J. of Remote Sensing* 20 (1):83-95.